

# Observation of coherent optical phonons in BiI<sub>3</sub>

著者	Mishina T., Masumoto Y., Fluegel B., Meissner K., Peyghambarian N.
journal or publication title	Physical review B
volume	46
number	7
page range	4229-4232
year	1992-08
権利	(C)1992 The American Physical Society
URL	<a href="http://hdl.handle.net/2241/98222">http://hdl.handle.net/2241/98222</a>

doi: 10.1103/PhysRevB.46.4229

# Observation of coherent optical phonons in $\text{BiI}_3$

T. Mishina and Y. Masumoto

*Institute of Physics, University of Tsukuba, Tsukuba, Ibaraki 305, Japan*

B. Fluegel, K. Meissner, and N. Peyghambarian

*Optical Sciences Center, University of Arizona, Tucson, Arizona 85721*

(Received 29 October 1991; revised manuscript received 11 March 1992)

Resonant coherent lattice vibrations in the vicinity of the indirect absorption edge in a  $\text{BiI}_3$  layered crystal are observed in a femtosecond pump-probe experiment. Coherent optical phonons that are impulsively excited by femtosecond pump pulses modulate the phase of probe pulses, causing oscillation of the probe spectrum in time. This oscillation, which has a period given by the period of the oscillation, continues for more than 100 cycles. We speculate that the coherent phonon-assisted indirect exciton transitions also contribute to the data.

Progress in ultrafast laser techniques has enabled direct observation of the coherent response of phonons and excitons. Coherent phonons can be impulsively generated by laser pulses whose temporal widths are shorter than the period of phonon oscillation.<sup>1</sup> The coherent phonon state is a coherent superposition of various number states of the relevant phonon mode. As excess numbers of phonons are populated in particular modes, the coherent phonon state is far from thermal equilibrium. By using ultrafast time-resolved techniques, coherent lattice vibrations and their damping have been directly observed in various materials.<sup>1-4</sup>

In this paper, we report the observation of ultrafast phase modulation caused by coherent phonon excitation in layered  $\text{BiI}_3$ .  $\text{BiI}_3$  belongs to a family of layered metal halides<sup>5</sup> consisting of strongly bonded two-dimensional layers with weak Van der Waals interlayer coupling. The structure gives the rigid-layer mode of lattice vibration,<sup>6</sup> which is expected to continue for a long time because of its low-energy oscillation and small damping. The optical-absorption edge of  $\text{BiI}_3$  is characterized by phonon-assisted indirect exciton transitions and very sharp exciton peaks, called the direct  $R$ ,  $S$ , and  $T$  excitons, due to stacking disorders in the crystal.<sup>5-8</sup> The indirect transition is that from the  $\Gamma$  point of the valence band to the  $Z$  point at the zone boundary of the conduction band. Both the direct as well as the indirect optical transitions may be affected by the coherent phonon oscillation. Thus,  $\text{BiI}_3$  is a unique material for studying the interaction between coherent lattice vibrations and excitonic transitions. The  $R$ ,  $S$ ,  $T$ , and the indirect exciton energies are located around 2 eV and are easily excited by available femtosecond dye lasers.

Our sample, with a thickness of  $\approx 10 \mu\text{m}$ , was grown by the sublimation method, under conditions of excess iodine in the gas phase. Figure 1 shows the absorption spectrum of the sample at 10 K. The  $R$ ,  $S$ , and  $T$  exciton absorption lines appear close to the fundamental absorption edge, as expected. The energy position of the indirect exciton is labeled  $E_{gx}^i$  in Fig. 1.

The Arizona laser system used in the experiment is composed of a balance colliding-pulse mode-locked laser and a six-pass dye amplifier pumped by a copper-vapor laser operating at 8.4 kHz. The temporal width of amplified output pulses was 64 fs after compensation of group-velocity dispersion by a double prism pair. The spectrum of the amplified pulses is centered at 1.99 eV and entirely covers the absorption lines of the  $R$ ,  $S$ , and  $T$  stacking-fault excitons, as shown in Fig. 1. The orthogonally polarized pump and probe pulses cross at the sample at an angle of about  $20^\circ$ .

In Fig. 2 the temporal traces of the absorption change at 10 K for four spectral positions are shown. The energy density of the pump pulses is about  $850 \mu\text{J}/\text{cm}^2$ , 30% of which is absorbed by the sample. Traces for the  $R$ ,  $S$ , and  $T$  excitons all show a rise at negative time delays and temporal oscillatory structure superimposed on the long-lasting bleaching component. The trace taken at the

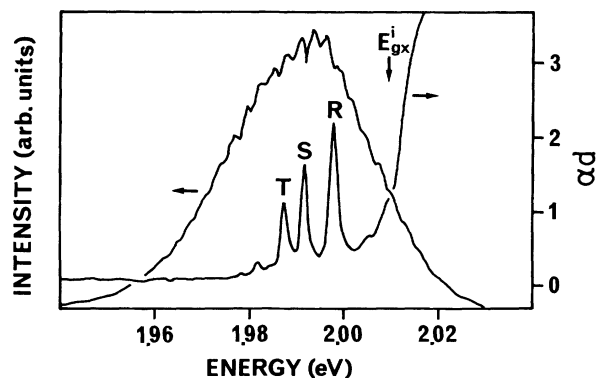


FIG. 1. Absorption spectrum of the  $\text{BiI}_3$  sample and the spectrum of the amplified laser pulses are shown.  $ad$  denotes the absorption coefficient  $\alpha$  multiplied by sample thickness  $d$ . The laser spectrum entirely covers the  $R$ ,  $S$ , and  $T$  exciton lines and the indirect exciton region. The indirect exciton energy is denoted by  $E_{gx}^i$ .

transparent region of the sample (1.97 eV) shows the temporal oscillation without bleaching. Furthermore, there is a phase shift between the oscillation observed in the four traces of Fig. 2, as evidenced by the vertical lines labeled *a* and *b*. The transmitted probe spectra taken for two time delays, shown by *a* and *b*, are displayed in the inset of Fig. 2. The spectral positions for the four temporal traces of Fig. 2 are marked by the arrows in the inset of Fig. 2. The transmission minima in the inset correspond to the *R*, *S*, and *T* excitons. While the exciton positions show no shift, the envelope of the transmitted spectrum clearly exhibits temporal oscillation. The oscillations of the probe spectrum are unambiguously seen in the temporal behavior of the differential signal in the transparent region (1.97 eV).

The negative time-delay signals observed for excitons in Fig. 2 are related to the optical coherence time  $T_2$  of the excitons.<sup>9</sup> It can be simply explained by noting that the transmitted intensity of the probe pulse is detected by a time-integrating detector. The polarization generated by the probe pulse in the sample persists for the optical coherence time  $T_2$  and is affected by the pump pulse that arrives at the sample after the probe pulse.

Figure 3(a) shows absorption changes at several negative time delays where the well-known spectral oscillatory structures around the *R*, *S*, and *T* excitons are observed.<sup>9</sup>

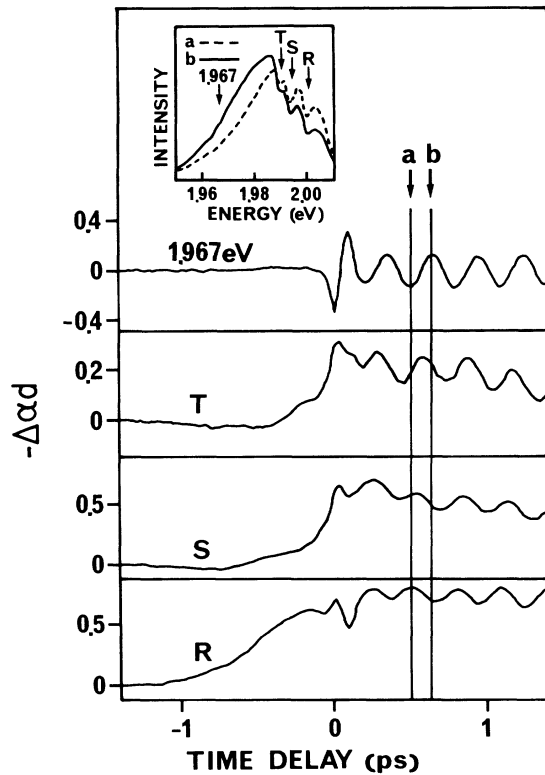


FIG. 2. Temporal traces of absorption change at four spectral positions, the *R*, *S*, and *T* excitons and transparent region 1.97 eV. The spectrum of the transmitted probe beam at two time delays *a* and *b* are displayed in the inset. Apparent spectral shift can be seen.

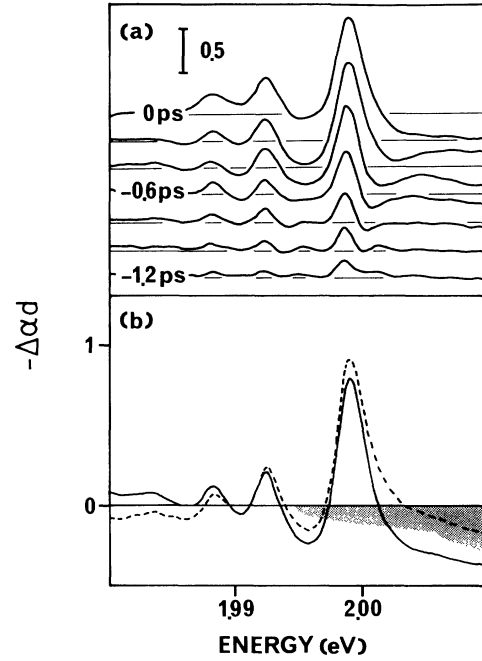


FIG. 3. (a) Absorption changes at several negative time delays. (b) Differential transmission spectra at two time delays. The shaded region corresponds to the one-phonon-assisted indirect transition. The spectral shape of the region is expressed by  $(E - E_{gx}^i + E_{op}^A)^{1/2} + (E - E_{gx}^i + E_{op}^C)^{1/2}$ , where  $E$  is the photon energy,  $E_{gx}^i$  is the indirect exciton energy, and  $E_{op}^A$  and  $E_{op}^C$  are the energies of *A*(*Z*) and *C*(*Z*) optical phonons, respectively.

As expected at positive time delays, the transient spectral oscillatory structures have vanished. In Fig. 3(b), where the differential transmission spectra for two time delays are plotted, we again observe that the entire spectral region covering the *R*, *S*, and *T* excitons and the transparency region oscillate in time. As we will show later in this paper, this temporal oscillation does not originate from an absorption change, but results from a refractive-index change. Also, an induced absorption region (where the  $-\Delta\alpha\Delta$  signal is negative), as displayed by the shaded area, is seen to coincide with the one-phonon-assisted indirect excitonic transition region. The absorption spectrum due to the thermal-phonon-assisted indirect transition has been extensively studied by Kaifu and Komatsu.<sup>5</sup> The induced absorption region is built up quickly at 0 fs and decays slowly. The *R*, *S*, and *T* lines show small broadening with no detectable energy shift as can be seen from Fig. 3(b). These observations cannot be explained by a temperature rise induced by the laser irradiation since such a temperature rise would be expected to cause an energy shift of the *R*, *S*, and *T* lines in addition to their broadening.<sup>8</sup>

Figure 4 shows the dynamics of the  $-\Delta\alpha\Delta$  signal at the *R* exciton for longer time delays, and its power spectrum obtained by numerical Fourier transformation after baseline subtraction. Two prominent peaks positioned at 0.6 and 3.4 THz, labeled *A* and *C*, appear in the spec-

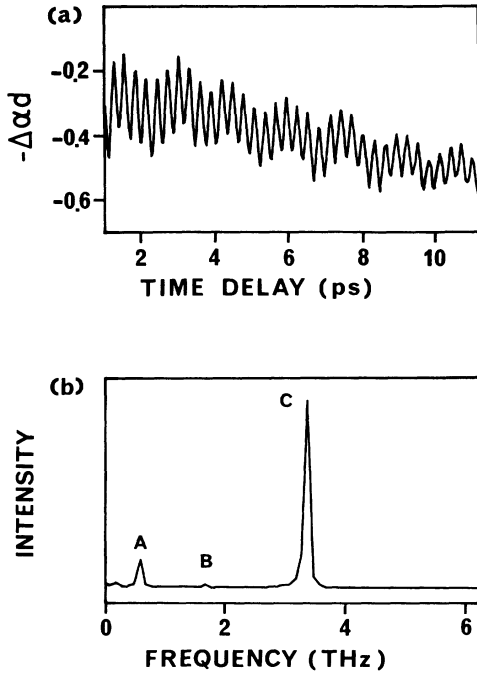


FIG. 4. Long-period temporal oscillation at the  $R$  exciton and its power spectrum obtained by the numerical Fourier transformation. The inclined baseline is subtracted from the temporal trace before the transformation. Three peaks appearing in the power spectrum are assigned to the phonon modes of  $A_g$  symmetry.

trum. An additional peak at 1.8 THz, labeled  $B$ , is also present with a much reduced strength. Raman-scattering experiments have revealed<sup>6,7</sup> three prominent Raman peaks with energy shifts of 22.8, 58.5, and 113.3  $\text{cm}^{-1}$ , corresponding to the phonon frequencies of 0.68, 1.75, and 3.40 THz, and being referred to as zone-center phonons  $A(\Gamma)$ ,  $B(\Gamma)$ , and  $C(\Gamma)$ , respectively.<sup>6,7</sup> The peaks are assigned to Raman-active modes at the  $\Gamma$  point belonging to the irreducible representation  $A_g$ . We also observed these peaks in the Raman spectrum of our sample, confirming prior measurements. Also, resonant Raman scattering, where the resonance is with respect to the indirect exciton energy,  $E_{gx}^i$  (with the incident photon energy being at  $E_{gx}^i$  plus the phonon energy), have shown the participation of the zone-boundary  $Z$  phonons.<sup>6</sup> The  $Z$  phonon energies are very close to the  $\Gamma$  phonon energies, being 20.8, 56.7, and 110.2  $\text{cm}^{-1}$  for the  $A(Z)$ ,  $B(Z)$ , and  $C(Z)$  phonons, respectively. As shown in Fig. 1, our laser spectrum covers not only the  $R$ ,  $S$ , and  $T$  excitons, but also the energy spectrum in the vicinity of the indirect exciton. Therefore, we expect that both  $\Gamma$  and  $Z$  phonons are coherently generated.

The observed temporal oscillations result from the time-dependent refractive index change induced by the strong incident femtosecond light pulses, impulsively generating coherent phonons. The coherent phonons modulate the refractive index. The phase of the light field after passing through the transparent material with time-

dependent refractive index  $n(t)$  is written as

$$\phi_{\text{out}} = \phi_{\text{in}} + n(t)d\omega_{\text{in}}/c, \quad (1)$$

where  $d$  is the thickness of the material,  $\phi_{\text{in}}$  and  $\omega_{\text{in}}$  are the phase and frequency of input light field, and  $c$  is the speed of light in vacuum. We assume  $n(t)$  oscillates continuously with a single frequency, given by

$$n(t) = n_0 + \Delta n \sin \Omega t, \quad (2)$$

where  $n_0$  is the linear refractive index,  $\Delta n$  is an oscillation amplitude of the refractive index, and  $\Omega$  is the frequency of oscillation. The frequency is given by a time derivative of the phase. Therefore, frequency of output light field  $\omega_{\text{out}}$  is written as

$$\omega_{\text{out}} = \omega_{\text{in}}(1 + d\Delta n\Omega \cos \Omega t / c). \quad (3)$$

The oscillation amplitude of the transmitted spectrum is  $\approx 4$  meV from Fig. 2. Using the experimental parameters in Eq. (3), a value of  $\Delta n = 3 \times 10^{-3}$  is obtained. The energy density of the pump pulses absorbed by the sample is  $255 \mu\text{J}/\text{cm}^2$ .

The probe spectral shift is proportional to the time differential of the phonon-modified refractive index. Thus, the Fourier transform of the time-domain data gives the phonon spectrum. The effect of propagation delay is reasonably omitted—since the pump and probe pulses travel in the same direction, they require the same time delay to reach a respective layer. Therefore, relative timing of the pump and probe pulses is the same at every layer.

In Fig. 5, we show the dynamics of the  $-\Delta\alpha d$  signals for the transparency region of the sample at 1.967 eV for various time domains, including the very long times, exhibiting the damping of the induced oscillations. The dominant oscillation with a  $\sim 300$ -fs period is clearly observed to continue for more than one hundred periods.

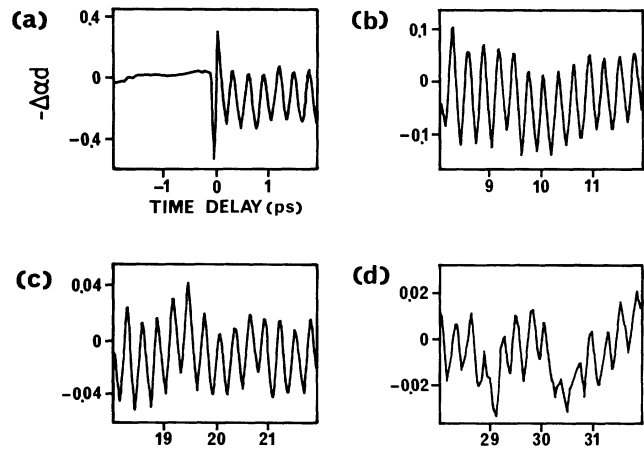


FIG. 5. The relaxation of coherent phonon oscillation at transparent region. The dominant oscillation ( $\sim 300$ -fs period) continues for more than one hundred periods. At longer time delay, the slow but long-lived oscillation (1.5-ps period) becomes dominant.

In addition, we have seen a slower but long-lived oscillation with a period of  $\sim 1.5$  ps. This long-lived 1.5-ps-period oscillation was seen in Raman-scattering experiments and has been assigned to the rigid layer mode by Komatsu, Karasawa, and Kaifu.<sup>6</sup>

In the presence of coherent phonons, the *R*, *S*, and *T* lines show a small broadening, but no detectable shift and no phonon side bands. In this sense, the stacking-fault direct excitons are affected only slightly by the generated coherent optical phonons. On the other hand, a prominent induced absorption band, which is observed above the energy of indirect exciton minus the *Z* point phonon energies of 20.8 and 110  $\text{cm}^{-1}$ , implies that the indirect transitions are strongly coupled with coherent phonons. We speculate that this induced absorption is associated with a strong coherent phonon-assisted transition. It is noted that the position of the laser frequency with respect to the absorption edge of the  $\text{BiI}_3$  is also important for the efficient coherent phonon effect. Since our laser spectrum covers the absorption edge, we think that resonant enhancement contributes to both generation and detection of coherent phonons. A detailed study in both

theoretical and experimental aspects is needed to clarify these interactions further.

In conclusion, coherent phonon oscillation is observed in a layered compound  $\text{BiI}_3$  by a femtosecond pump and probe technique. Coherent phonons cause ultrafast phase modulation through the change in refractive index. A distinct spectral shift of the transmitted probe pulses was observed. The coherent phonon oscillation continues for more than one hundred periods. The Fourier analysis of the temporal trace reveals three frequency components that correspond to the Raman-active optical phonons. The interaction of coherent phonons with indirect excitons appears to cause an induced absorption.

This work was supported by the NEDO (New Energy and Industrial Technology Development Organization) of Japan, and the International Science Research Program (Grant No. 02044021) from the Ministry of Education, Science and Culture, Japan (MESC). The Arizona group was also supported by the United States National Science Foundation and the United States Army Research Office.

<sup>1</sup>S. De Silvestri, J. G. Fujimoto, E. P. Ippen, E. B. Gamble, Jr., L. R. Williams, and K. A. Nelson, *Chem. Phys. Lett.* **116**, 146 (1985).

<sup>2</sup>W. E. Bron, J. Kuhl, and B. K. Rhee, *Phys. Rev. B* **34**, 6961 (1986).

<sup>3</sup>G. C. Cho, W. Kütt, and H. Kurz, *Phys. Rev. Lett.* **65**, 764 (1990).

<sup>4</sup>J. M. Chwalek, C. Uher, J. F. Whitaker, G. A. Mourou, and J. A. Agostinelli, *Appl. Phys. Lett.* **58**, 980 (1991).

<sup>5</sup>Y. Kaifu and T. Komatsu, *J. Phys. Soc. Jpn.* **40**, 1377 (1976); see also Y. Kaifu, *J. Lumin.* **42**, 61 (1988).

<sup>6</sup>T. Karasawa, T. Komatsu, and Y. Kaifu, *Solid State Commun.* **44**, 323 (1982); see also T. Komatsu, T. Karasawa, T. Iida, K. Miyata, and Y. Kaifu, *J. Limin.* **24&25**, 679 (1981); see also T. Karasawa, T. Iida, M. Sasaki, T. Komatsu, and Y. Kaifu,

*J. Phys. C* **18**, 4043 (1985).

<sup>7</sup>Y. Petroff, P. Y. Yu, and Y. R. Shen, *Phys. Status Solidi B* **61**, 419 (1974).

<sup>8</sup>K. Watanabe, T. Karasawa, T. Komatsu, and Y. Kaifu, *J. Phys. Soc. Jpn.* **55**, 897 (1986).

<sup>9</sup>B. Bluegel, N. Peyghambarian, G. Olbright, M. Lindberg, S. W. Koch, M. Joffre, D. Hulin, A. Migus, and A. Antonetti, *Phys. Rev. Lett.* **59**, 2588 (1987); see also M. Joffre, D. Hulin, A. Migus, A. Antonetti, C. Benoit a la Guillaume, N. Peyghambarian, M. Lindberg, and S. W. Koch, *Opt. Lett.* **13**, 276 (1988); see also M. Lindberg and S. W. Koch, *Phys. Rev. B* **38**, 7607 (1988); see also J. P. Sokoloff, M. Joffre, B. Fleugel, D. Hulin, M. Lindberg, S. W. Koch, A. Migus, A. Antonetti, and N. Peyghambarian, *ibid.* **38**, 7615 (1988).

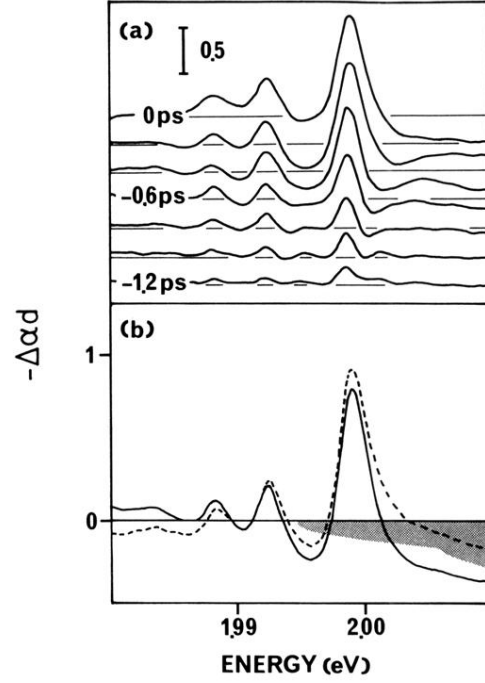


FIG. 3. (a) Absorption changes at several negative time delays. (b) Differential transmission spectra at two time delays. The shaded region corresponds to the one-phonon-assisted indirect transition. The spectral shape of the region is expressed by  $(E - E_{gx}^i + E_{op}^A)^{1/2} + (E - E_{gx}^i + E_{op}^C)^{1/2}$ , where  $E$  is the photon energy,  $E_{gx}^i$  is the indirect exciton energy, and  $E_{op}^A$  and  $E_{op}^C$  are the energies of  $A(Z)$  and  $C(Z)$  optical phonons, respectively.